Journal of the Geological Society, London, Vol. **159**, 2002, pp. 557–575. Printed in Great Britain.

Granite production in the Delamerian Orogen, South Australia

J. D. FODEN[1], M. A. ELBURG[1], S. P. TURNER[2], M. SANDIFORD[3], J. O'CALLAGHAN[1] & S. MITCHELL[1]

[1]*Department of Geology and Geophysics, Adelaide University, Adelaide, S.A. 5005, Australia, (e-mail: john.foden@adelaide.edu.au)*

[2]*Department of Earth Sciences, University of Bristol, Bristol, UK*

[3]*School of Earth Sciences, University of Melbourne, Melbourne, Vic. 3010, Australia*

Abstract: In the South Australian sector of the Cambro-Ordovician Ross–Delamerian Orogen, granites range in age from Mid-Cambrian to Early Ordovician. Their occurrence is largely confined to deep, Early Cambrian, sediment-filled basins where they are associated with mafic rocks. The syntectonic suites have compositions forming a continuum between I- and S-type granites. After the cessation of convergent deformation at *c.* 490 Ma an abrupt transition to a bimodal magmatic association of mafic intrusions and felsic granites and volcanic rocks of S- and A-type affinities occurred. As exposed on the south coast of Kangaroo Island, S-type granite originated as *in situ* partial melts of the Early Cambrian sediments locally intruded by either mafic magmas or I–S granite magmas. These migmatite complexes were mingled with intrusions from the magmas that provided the underlying heat sources. Also on Kangaroo Island, composite S-type rhyodacite–dolerite dykes indicate that crustal melting involved mantle-derived melts. Field observations, major and trace element data and Nd–Sr isotopic data indicate that granite magmas in this fold belt result from mixing of crustal and mantle source components, and from fractional crystallization (AFC-type processes). Whereas the Nd–Sr compositions of granite suites from the Delamerian Orogen form a continuous geochemical trend between the crust and the mantle melts, the A- and I-types cluster towards the mantle endmember and the S-types towards the crustal endmember. This dichotomy reflects three granite magma production situations: (1) lower-crustal mafic magma chambers that are contaminated by, and mingled with, melts of the local metasediments producing I-type magmas; (2) crustal melts formed in the heated zones above upwelling mantle or close to mafic or I-type granite intrusions producing S-type magmas; (3) upper-crustal mafic intrusions where closed-system fractionation dominates to produce A-type granite. The extent of fractionation and crustal assimilation varied progressively through the *c.* 30 Ma deformation history (514–485 Ma) of this orogen. Importantly in this sector of the Ross–Delamerian Orogen, the crustal endmember is represented only by the Cambrian basin sedimentary fill (Kanmantoo Group) and expressly excludes the older Precambrian crust.

Keywords: AFC, South Australia, Ross–Delamerian Orogen, S-type granites, neodymium isotopes.

This paper concerns the origins of granite magmas in the Delamerian Fold Belt in South Australia (Table 1). When formed, this orogen was contiguous with the Ross Orogen in Antarctica, forming the earliest stage of development of the Tasman Orogen and lying between the western edge of the younger Palaeozoic Lachlan Fold Belt and the Precambrian Craton (Coney *et al.* 1990). The dispute over the origin of granite, particularly in the Lachlan Fold Belt, has been considerable and encapsulates debate repeated in many other global granitic terranes (Chappell & White 1974, 1992; White & Chappell 1988; Chappell 1996; Collins 1998). The terms I- and S-type granite were coined there (Chappell & White 1974, 1992; White & Chappell 1988) and likewise the concept of restite (Chappell *et al.* 1987; Chappell 1996). These models led to granites being regarded as simple geochemical 'images' of their sources and essentially intracrustal phenomena. The contrary view, however, is that granite is a mixture of crustal and mantle sources (Gray 1984; Collins 1998).

In this paper we use the granites of the Delamerian Orogen to contribute another dimension to this debate, particularly taking advantage of the extensive knowledge of the rocks that form the basement to this fold belt compared with that of the Lachlan Fold Belt.

Regional geological setting

The Cambro-Ordovician Delamerian Orogen in the southern Adelaide Fold Belt (Figs 1 and 2) (Preiss 1987; Jenkins & Sandiford 1992) lies directly to the east of the Precambrian craton and hosts granitic rocks and felsic volcanic rocks with ages in the range *c.* 520 Ma to 480 Ma. In South Australia this orogen underwent deformation from early Mid-Cambrian (514 ± 4 Ma; Foden *et al.* 1999) to Early Ordovician time (*c.* 490 Ma). This Cambrian activity is concurrent with subduction-related arc volcanism *c.* 1000 km to the east in the Takaka Terrane in New Zealand (Fig. 1) (Münker & Cooper 1995; Münker & Crawford 2000). The southern Adelaide Fold Belt is important as it marks the initiation of the major tectonic transition of the eastern margin of the newly assembled Gondwanan supercontinent, from Late Neoproterozoic passive margin, to Early–Mid-Cambrian convergent subduction margin (Coney *et al.* 1990; Powell *et al.* 1994). The latter state has prevailed from this time to the present, with progressive eastwards migration of orogenic activity through time. The Cambro-Ordovician Delamerian Orogen is bounded to its east by the Mid- to Late Palaeozoic Lachlan Fold Belt (e.g. Coney *et al.* 1990; Figs 1 and 2).

Table 1. *Cambro-Ordovician granites, Adelaide Fold Belt*

Granite name	Locality	Lat., long. (°)	Rock types	References
Syntectonic I- and S-type granites				
Remarkable Rocks	SW Kangaroo Is.	36.03, 136.45	grd–gran	2, 3
Cape Younghusband	SW Kangaroo Is.	36.02, 136.50	grd–gran	3
Vivonne Bay	West of Point Ellen, KI	36.02, 137.11	grd–gran	3
Stun Sail Boom River		36.02, 137.01	grd–gran	
Cape Willoughby	East Kangaroo Is.	35.52, 138.07	gran	2, 3
Victor Harbor–Port Elliot	Encounter Bay	35.35, 138.40	dior–gran	2, 3
Taratap Adamellite	SE South Australia	36.40, 139.50	adamellite	2
Monarto Granite	West of Murray Bridge	35.05, 139.10	gran	2, 3
Reedy Creek Granodiorite	Reedy Creek	34.55, 139.13	dior–gran	2
Palmer Granite	Palmer	34.52, 139.10	gran	2, 6
Rathjen Gneiss	North of Palmer	34.45, 139.08	grd–gran	6, 7
Tanunda Granite	East Barossa Valley	34.34, 139.00	grd–gran	7
Cookes Hill Granite	West of Sedan	34.45, 139.12	tonalite	9
Anabama Granite	South of Broken Hill	32.50, 140.10	dior–grd	9
Bungalina Monzonite	Peake and Denison Ranges	28.30, 136.00	monz–sy	8
Harrow Granite	West Victoria	37.18, 141.42	gran	1, 4, 5
Wando Granodiorite	West Victoria	37.28, 141.24	dior–gran	1, 4, 5
Post-tectonic A-type granites				
Black Hill	Cambria, West Murray Valley	34.41, 139.28	gab, monz, gran	1, 2, 3
Sedan Granite	Sedan, West Murray Valley	34.30, 139.21	gran	1
Mannum Granite	Mannum	34.53, 139.21	gran	1
Reedy Creek Diorite	Reedy Creek	34.55, 139.13	dior	1
Murray Bridge Granite	Murray Bridge	35.07, 139.10	gran	1
Mt Monster Porphyry	Mt Monster, SE South Australia	36.14, 140.21	ignimbrite	1
Padthaway Ridge–Coonawarra	Numerous small inliers in SE South Australia	35.45, 139.30 37.00, 140.45	gran–sy	1
Derholm Granite	West Victoria	37.25, 141.20	gran	1, 2, 5

References: 1, Turner *et al.* (1992); 2, Foden *et al.* (1990); 3, Milnes *et al.* (1977); 4, Flöttmann *et al.* (1994); 5, Gibson & Nihill (1992); 6, Fleming & White (1984); 7, Foden *et al.* (1999); 8, Morrison & Foden (1990); 9, Preiss (1987). Abbreviations: grd, granodiorite; gran, granite; dior, diorite; monz, monzonite; sy, syenite; gab, gabbro.

The Delamerian Orogeny

The southern Adelaide Fold Belt is part of a Neoproterozoic to Early Palaeozoic orogen that extended over 5000 km along the southeastern edge of the early Gondwana supercontinent (e.g. Dalziel 1991; Moores 1991). It is composed of mainly Neoproterozoic (Adelaidean) and Lower Cambrian (the Normanville and Kanmantoo Groups) sedimentary rocks with associated mafic igneous and granitic rocks (e.g. von der Borch 1980; Preiss 1987).

The Delamerian Orogen is a compressional orogen developed by westward vergent folds and thrust faults. Its structural history has been described by Offler & Fleming (1968), Fleming & White (1984), Mancktelow (1990), Jenkins & Sandiford (1992) and Flöttmann *et al.* (1994). Recent studies (Flöttmann *et al.* 1998, 1995, 1994) have recognized that the Kanmantoo sedimentary basin with its associated basalts and dolerites (Foden *et al.* 2002) formed as a localized steep-sided tear basin resulting from dextral shear on an east–west fault system south of Kangaroo Island (Fig. 2). As the Cambro-Ordovician mafic and felsic magmatism (Table 1) was largely confined to this Cambrian sedimentary trough it seems that early rifting was a very important stage in the evolution of the fold belt. It resulted in mantle exhumation and in the localization of zones of thermal interaction between crust and mantle.

The maximum age of commencement of the Normanville–Kanmantoo sedimentation and the age of onset of the Delamerian folding are constrained by U–Pb dating of zircons. Tuff layers in the basal Normanville Group yielded an Early Cambrian age of 526 Ma (Cooper *et al.* 1992), and the age of onset of deformation and the termination of sedimentation is provided by the age of the earliest syndeformational Rathjen Gneiss (514 Ma; Foden *et al.* 1999). These results indicate that the southern Adelaide Fold Belt evolved very quickly from sedimentary basin to fold belt and that the pre-deformational phase of Cambrian sedimentation and mafic magmatism lasted only *c.* 12 Ma.

The Delamerian Orogen is characterized by a low-*P* and high-*T* metamorphism (Offler & Fleming 1968; Mancktelow 1990; Dymoke & Sandiford 1992; Sandiford *et al.* 1992), showing large variation from chlorite to sillimanite grade, with the highest grades restricted to a narrow meridional belt, which is also the site of syntectonic granite intrusion and structural complexity. Assemblages indicate peak metamorphic conditions in the region of 0.3–0.4 GPa at temperatures up to 650 °C (Sandiford *et al.* 1990).

The termination of convergent deformation of the Delamerian Orogen is marked by the transition from deformed to undeformed granitoid intrusions, and U–Pb zircon dating (Turner & Foden 1996) as well as new Rb–Sr geochronology reported in this paper indicates that this transition took place at *c.* 485 Ma (see Table 5, below). Significantly, this transition is marked by major changes in the composition of granite magmas, from syntectonic I–S types to highly siliceous, potassic, post-tectonic A-types (Foden *et al.* 1990; Turner *et al.* 1992; Turner 1996; Turner & Foden 1996). These late-stage A-type felsic magmas form part of a high-temperature, bimodal magmatic suite generated after a phase of major uplift and erosion of the Delamerian Fold Belt (Turner *et al.* 1996). Nd-isotope and muscovite Ar/Ar provenance studies of sedimentary rocks support the observation that uplift and erosion of the Ross–Delamerian Orogen supplied

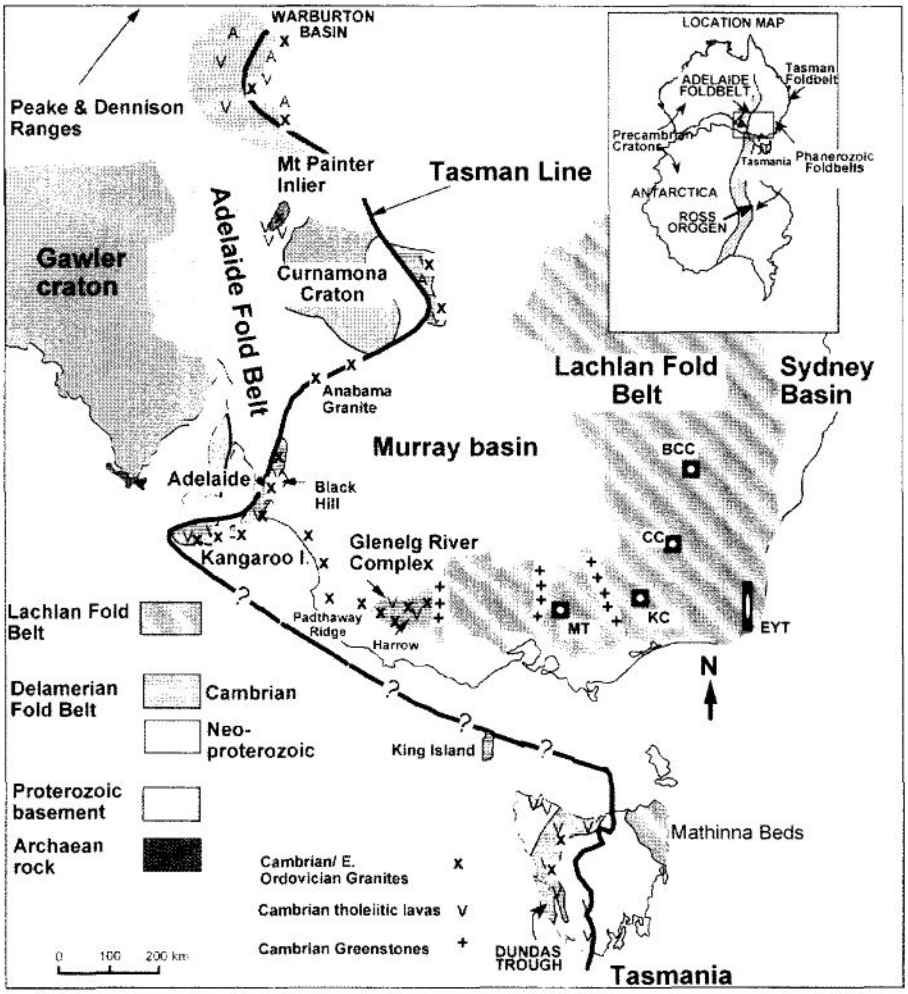

Fig. 1. Regional geological map showing the pre-Australia–Antarctic breakup configuration of the Delamerian and Ross Orogens. MT, Mansfield–Melbourne Trough; KC, Kuark Complex; CC, Cooma Complex; BCC, Bradley's Creek Complex; EYT, Eden Yalwal Trough

the extensive Lachlan Fold Belt Ordovician quartzose flysch deposits (e.g. Cas 1983; Fergusson *et al.* 1989; Turner *et al.* 1996).

Analytical methods

Clean fresh fragments of samples were crushed and then ground in a WC mill to $< 2\ \mu m$ grain size. This material was used for XRF and Sr and Nd isotopic analyses. XRF analyses were performed at the Department of Geology and Geophysics, Adelaide University, with a Philips PW1480 100 kV spectrometer using techniques described by Turner *et al.* (1993b) and Foden *et al.* (1999). Sr and Nd isotope ratios were analysed at the Department of Geology and Geophysics on either the Finnigan 261 single-collector, thermal ionization mass spectrometer (TIMS) in dynamic mode, or on the Finnigan MAT 262 TIMS in static mode. Methods have been described by Turner *et al.* (1993b) and Foden *et al.* (1999). During the interval over which analysis was undertaken the in-house Nd standard (J and M specpure Nd_2O_3) gave 0.511604 ± 9 (1σ of total population, $n = 105$), the La Jolla standard gave 0.511842 ± 15 and BCR-1 yielded 0.512636 ± 16. Blanks are in the order of 100–200 pg for Nd. The average for the NBS987 Sr standard is 0.710242 ± 12 ($n = 56$) and Sr blanks are better than 2 ng. The $^{143}Nd/^{144}Nd$ composition of CHUR was taken as 0.512638 and $^{147}Sm/^{144}Nd$ as 0.1967.

The Delamerian granites

This paper focuses on the Delamerian S-type granites (Tables 2 and 3) and particularly uses the Kangaroo Island exposures to develop an understanding of their origins and their relationship to the Delamerian I-type granites (Table 2). We also emphasize that the belt includes post-tectonic A-type granites (Turner *et al.* 1992), which are very important to the interpretation and understanding of the geochemical variation of the entire Delamerian granites series.

The syntectonic to earliest post-tectonic Delamerian granitoids range from I-type to S-type granite. The I-types are biotite- and/or hornblende-bearing, often titanite-bearing, plagioclase-rich diorite, tonalite, granodiorite and granite. The S-types are biotite-rich, hornblende-free, muscovite-bearing granite to granodiorite. The granites occur as relatively small and scattered outcrops on Kangaroo Island (Table 3, Figs 2 and 3) and northwards along the axis of the fold belt, to Mt Painter and the Peake and Denison Ranges in the far north (Fig. 1). They are confined to the Cambrian basin or to fault structures active during Cambrian time. Although exposed granite outcrops are small and scattered, recent high-resolution total magnetic intensity (TMI) imagery reveals that both syn- and post-tectonic granite intrusions are much more extensive to the east of the Mt Lofty Ranges in the Murray Basin, which is floored by Cambrian rocks beneath Mesozoic cover. The syntectonic granites (e.g. the Rathjen

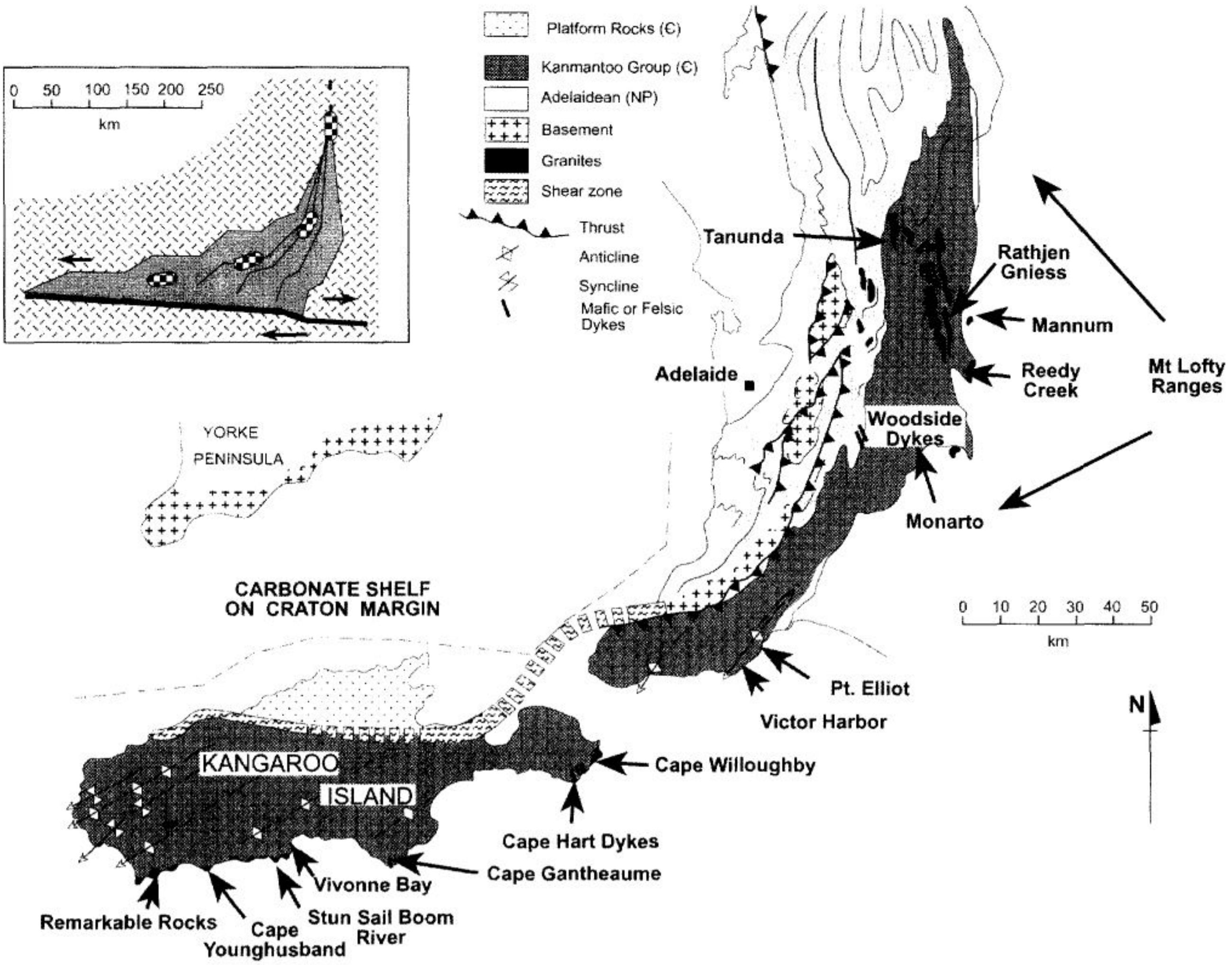

Fig. 2. A more detailed map of the southern Adelaide Fold Belt showing the granites and the locality of geographical and geological features mentioned in the text. The inset shows the postulated configuration of the Kanmantoo basin developed as a tear basin as proposed by Flöttmann *et al.* (1998); stippling, Precambrian basement rocks; dark grey, Kanmantoo basin fill; checked pattern, granites.

Gneiss; Foden *et al.* 1999) are I- to S-type and have tectonic fabrics, metamorphic halos (with staurolite–cordierite–andalusite assemblages) and were emplaced at middle upper-crustal levels (*c.* 12 km) between 516 and 490 Ma. With this series we also include the deformed granites and associated dioritic–granodioritic rocks (the Wando granites) in the western Victorian Glenelg Province, regarding this as a geologically equivalent terrane (Gibson & Nihill 1992; Turner *et al.* 1993a). The compositional relationships between the three granite series are summarized in Figs 4 and 5. Although dominated by I-type, there are also peraluminous S-type granites that are sometimes migmatitic (Fig. 3). Examples of these occur at Vivonne Bay–Stun Sail Boom River in southern Kangaroo Island (Fig. 2) or at Harrow (Figs 1 and 2) in western Victoria (Turner *et al.* 1993a).

Kangaroo Island

Southern Kangaroo Island provides exposures that give us particularly good insight into the origin of S-type granite in the South Australian sector of the Delamerian belt. These data also provide good evidence for the origin of a component that clearly has been involved in the evolution of I-type granites throughout the belt.

The Cape Willoughby granite. The Cape Willoughby granite has contacts exposed on the northeastern and southeastern coasts and appears to be a roughly layer-parallel sheet-like intrusion into the host Kanmantoo Group turbiditic sediments. This granite has been dated at 509 ± 7 Ma by sensitive high-resolution ion microprobe (SHRIMP) U–Pb analysis of zircons (Fanning 1990). The granite has evolved thin, leucocratic, sill-like apophyses, which also intrude the host sequence layer parallel and which are boudinaged. The Cape Willoughby granite (Table 2) is a mildly peraluminous, leucocratic, siliceous (> 75% SiO_2) S-type granite. It is composed of quartz, K-rich microcline and relatively scarce plagioclase, muscovite and biotite. It is clearly a fractionated granite and has low MgO, CaO, FeO*, TiO_2, P_2O_5, Zr, Sr and REE, and is moderately rich in K_2O, Rb and U.

The Vivonne Bay–Stun Sail Boom River Migmatite Complex. At these localities the Kanmantoo Group is intruded by a K-feldspar megacrystic biotite granite of transitional I- to S-type composi-

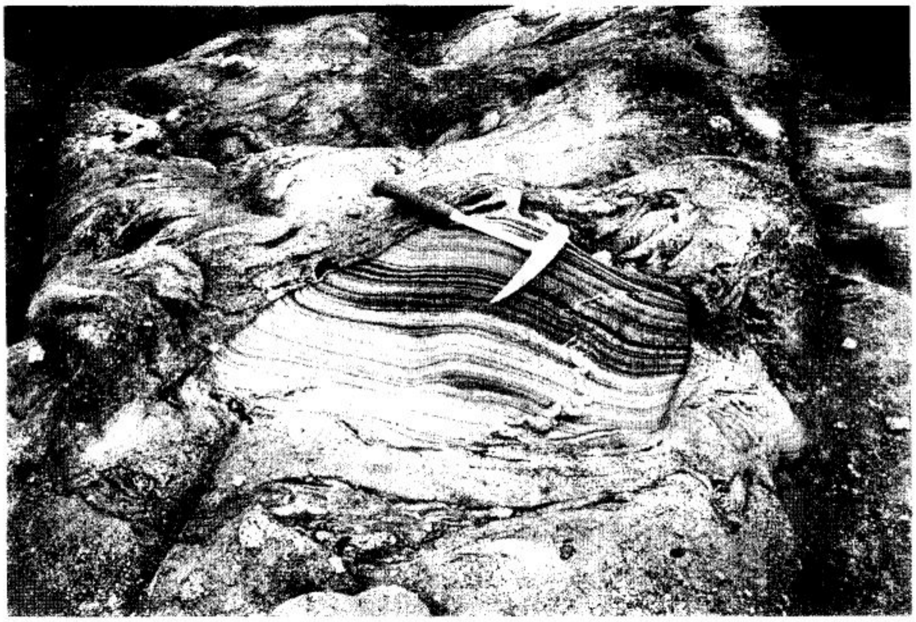

Fig. 3. Field photograph showing detail of the biotite granodiorite diatexite at Vivonne Bay–Stun Sail Boom River. Hammer for scale (35 cm).

tion (Table 2). This granite has limited on-land exposure and crops out at a series of headlands between Vivonne Bay and Remarkable Rocks 30 km to the west (Fig. 2). At the Vivonne Bay–Stun Sail Boom River localities, the host Kanmantoo Group metasedimentary rocks are metamorphosed to upper amphibolite facies and are partially melted to produce a locally mobilized diatexitic biotite granodiorite (Fig. 3, Table 2). This granodiorite is fairly biotite rich and is host to numerous enclaves of unmelted Kanmantoo Group metasediments (Fig. 3). These enclaves are clearly of lithologies that were less favourable for melt production at the prevailing temperatures and comprise both quartz-rich lithologies and also very biotite-rich melanosome fragments. These latter are the same composition as some *in situ* melanosome layers bordering the biotite granodiorite and are composed of biotite, plagioclase (An_{34-12}), minor quartz and abundant accessory apatite, zircon and monazite.

The locally produced biotite granodiorite melt was obviously contemporaneous with the megacrystic granite intrusion, as there are good examples of mingling of fingers of the porphyritic granite with the grey biotite granodiorite. The biotite granodiorite has a moderately developed foliation, which defines approximately northerly dips of 30–50°. Development of the migmatite complex and emplacement of the megacrystic granite (503 ± 4 Ma) are regarded as syn-Delamerian orogenic events.

In addition to the megacrystic granite and the biotite granodiorite, these outcrops also expose bodies of highly leucocratic granite (Table 2). These biotite-free rocks are composed of quartz, K-rich microcline and muscovite and contain numerous patches of almandine-rich garnet granite. These garnet leucogranites are seen locally to mingle with the biotite granodiorite and they are taken to represent extracted and fractionated near minimum-temperature melts. The occurrence of muscovite as a solidus phase in these liquids constrains their pressure to be above 3 kbar (e.g. Dymoke & Sandiford 1992). This granite has been dated at 504 ± 8 Ma by SHRIMP U–Pb analysis of zircons (Fanning 1990). In this paper we also present new, two mica–apatite, internal Rb–Sr isochron data pointing to an age of 487.4 ± 3.5 Ma for this complex, probably reflecting the age of cooling below 350 °C (Table 5).

The three rock types exposed at these localities have the following geochemical features.

(1) The diatexites range from biotite granodiorite to granite (Table 2) with between 62 and 75% SiO_2. These show linear geochemical relations on Harker diagrams (see Fig. 7, below), and with increasing silica content show depletion in most elements including La, Ce, Nd, Zr, MgO, FeO*, CaO, P_2O_5, Na_2O, TiO_2, V, Sc, Cr and Ni. They also show enrichment in K_2O, Rb, Th and U. ASI values decrease with increasing silica. These granites have the same characteristics as the S-type granites and granodiorites from the Lachlan Fold Belt (White & Chappell 1988; Elburg & Nicholls 1995; Elburg 1996), with relatively low Na_2O and CaO. Likewise, when also compared with I-types they have high Mg-number numbers and relatively high V, Cr and Ni at given silica levels. In keeping with the known elevated phosphorus solubility in peraluminous melts (e.g. Bea *et al.* 1992) they are also characterized by somewhat elevated P_2O_5 levels at given silica levels. The linear array of the diatexites also includes the biotite melanosome rocks. Compared with the diatexites, the intrusive porphyritic (megacrystic) granite is more siliceous on average and has lower ASI (Figs 5 and 7). Also in comparison with the diatexite series the intrusive porphyritic granites are distinguished by their curving trends of more pronounced depletion in MgO, CaO and most trace elements (except for Rb and U) with increasing silica (see Fig. 8, below). These trends have the garnet leucogranite (see Fig. 8) as their endpoint.

(2) The biotite melanosome (Table 2) rocks occur both as enclaves distributed through the biotite granodiorite and in the marginal zones of the granite sheets. These rocks are composed of dominant biotite, with plagioclase, quartz, apatite and accessory zircon, allanite and monazite. They have high K_2O, MgO, FeO*, Rb, Ba, V, Cr and Ni, low SiO_2, Na_2O and CaO, and high ASI values (> 1.5). These rocks also contain very high light REE (LREE) and U, reflecting the role of monazite as a sink for some incompatible elements (Table 2).

(3) The garnet leucogranites (Table 2) formed as siliceous (75% SiO_2), mafic-mineral-poor segregated melt bodies adjacent to the biotite granodiorite. They are very MgO and CaO poor and have ASI values close to 1.1. In comparison with the biotite granodiorite (Figs 6 and 8) the leucogranites are depleted in Ba, Th, U, Nb, the REE, Sr, Zr, Ti, Y, V, Sc, Cr and Ni. They have similar Rb, K and Pb levels, are slightly enriched in P_2O_5, and

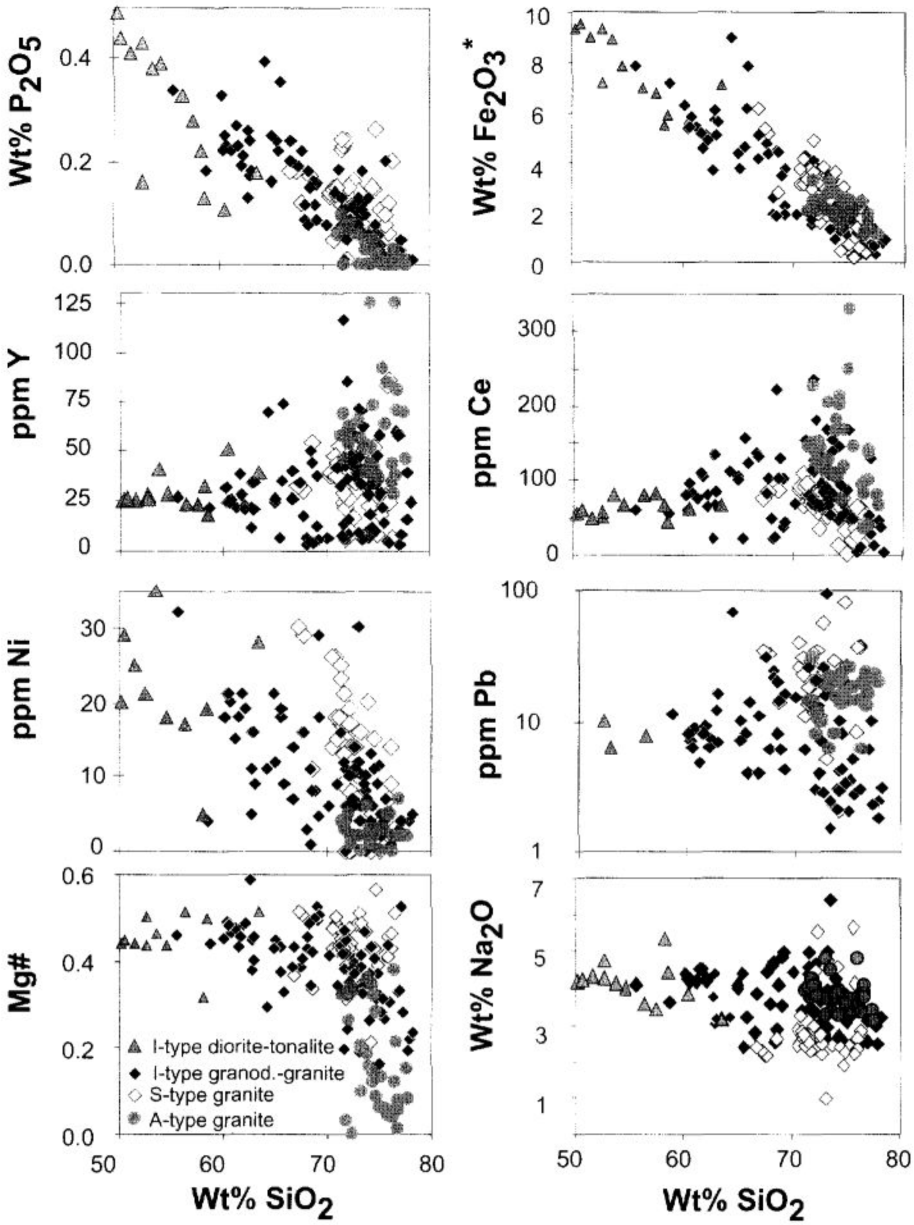

Fig. 4. Selected Harker geochemical variation diagrams illustrating the general regional geochemical relationships amongst the Delamerian granite suites. Shaded triangles, I-type diorites and tonalite from the South Australian Reedy Creek and Anabama plutons and Wando Vale (near Harrow in western Victoria); ◆, Cambrian I-type granites from the South Australian and Victorian Delamerian intrusions; ◇, S-type granites from the South Australian and Victorian Delamerian intrusions; shaded circles, A-type granites from the South Australian and Victorian late Delamerian intrusions.

have higher U/Th ratios. As illustrated by the MgO v. SiO_2 variation diagram (Fig. 8) the composition of the garnet leucogranites is not collinear with the trend of the biotite granodiorite and these melts can therefore not be considered as the end-member melt of the restitic trend that seems to control compositional variation in those rocks.

The Cape Hart–Cape Gantheaume composite dykes. More than 20 dykes have been identified cutting the deformed Kanmantoo sequence on the SE coast of Kangaroo Island (Fig. 2). These have a strongly clustered NW (325°) orientation and are vertically dipping. The Kangaroo Island dykes appear largely to post-date the Delamerian folding and contain no tectonic fabric or, rarely, a weak cross-cutting one. Although the early regional fabrics that are cross-cut are in different orientations, the Kangaroo Island dykes have exactly the same orientation as the dolerite dyke swarm at Woodside (Table 3) further north in the belt, about 50 km east of Adelaide (Fig. 2). With their implication of a common dilation direction, we attribute both dyke complexes to the onset of the first stages of post-Delamerian broadly eastward extension. These dykes have been dated at Cape Gantheaume (Fig. 2) at 500 ± 7 Ma by SHRIMP U–Pb analysis of zircons (Fanning 1990).

The Kangaroo Island dykes are between 0.5 and 4 m wide and are interesting because most are composite, with mafic and felsic (rhyodacite) components (Table 3). A few are either entirely mafic or felsic. The dykes commonly show mafic borders with felsic interiors, implying initial injection of mafic melts. In most composite dykes we also see mingling between the felsic and mafic magmas, the rhyodacite hosting convolute–amoeboid enclaves of basaltic melt, indicating that the two melts were contemporaneous.

The felsic dyke rocks (Table 3) are porphyritic with rounded and embayed quartz phenocrysts together with phenocrysts of plagioclase and K-feldspar. These are set in a fine, dark, recrystallized matrix. The mafic dyke rocks have plagioclase intergrown with augite (mostly replaced by amphibole) in a doleritic texture.

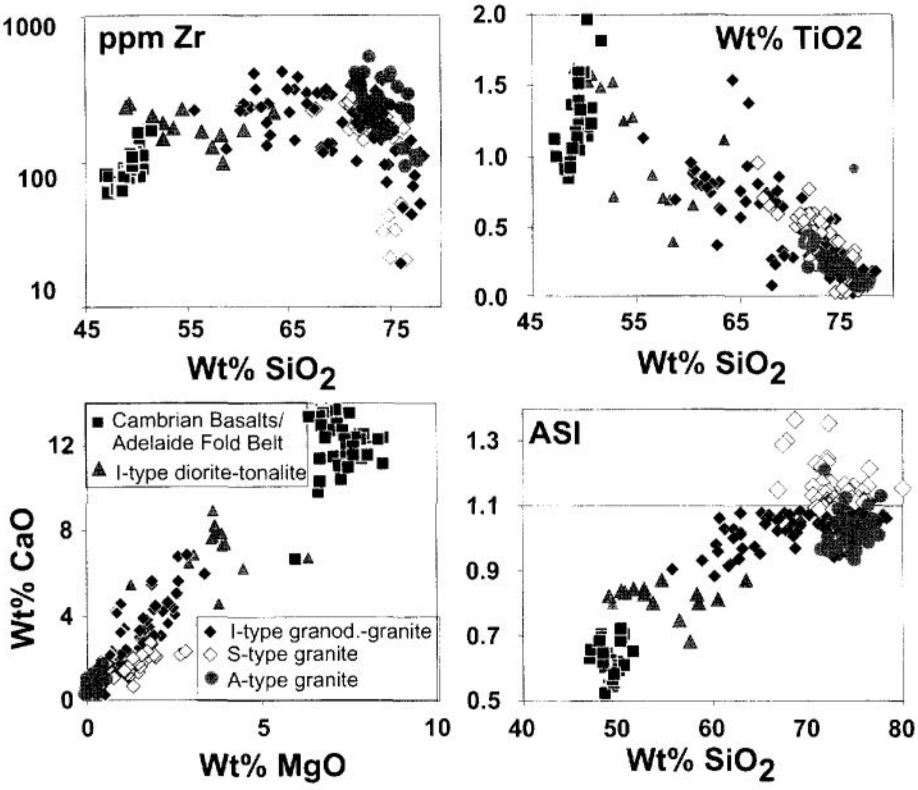

Fig. 5. Selected Harker diagrams and CaO v. MgO covariation illustrating the relationship between the regional compositional variation of the Delamerian granites and the composition of Cambrian basalts from the belt. Symbols as in Fig. 4; ■, Cambrian basalts from the Delamerian belt (Foden *et al.* 2002). ASI, aluminium saturation index (molar $Al_2O_3/(Na_2O + K_2O + CaO)$).

The felsic components of the dykes have SiO_2 contents that range between 63.5 and 73.5%. At the more felsic end of this spectrum they have compositions that are the same as those of the Vivonne Bay anatectic biotite granodiorites with about 72–73% SiO_2 or the megacrystic intrusive granite (Fig. 7, and see Fig. 11, below). The felsic component of the composite dykes, however, extends towards lower SiO_2, dacitic compositions with linear increases in CaO, MgO, FeO*, TiO_2, Ni, V, Cr and Sc, and with decreasing ASI values (Figs 7 and 11). These trends extend directly towards the mafic magmas and are most probably due to mingling and hybridization. This conclusion is further borne out by the Nd and Sr isotopic compositions, which show progressive variation as a function of changing bulk rock composition, appearing to mix between Kanmantoo Group type crustal values and the mantle values of the mafic rocks (Figs 7 and 9).

Nd- and Sr-isotope ratios

Nd- and Sr-isotopic data are presented in Table 4 and Figs 7, 9 and 10. The combined suite of I- and S-type granites shows widely variable isotopic compositions. They range from I-type granodiorite and tonalite, which differ strongly from Kanmantoo Group country rocks or any pre-Adelaidean basement, in having low initial $^{87}Sr/^{86}Sr$ ratios (*c.* 0.7060) and high initial ϵNd (+1 to −3), through to siliceous S-type granites including those at Victor Harbor (e.g. Milnes *et al.* 1977), Cape Willoughby or Vivonne Bay (Kangaroo Island), which have initial $^{87}Sr/^{86}Sr$ ratios in excess of 0.715 and ϵNd values as low as −13.

The wide variation in Sr- and Nd-isotopic compositions of the syn- to late orogenic I and S-type granites is also partly correlated with major and trace element variations (Fig. 10). The Nd- and Sr-isotopic composition of the I-type granites falls between the contemporary mafic magmas from the belt and the field of S-type granite (Figs 9 and 10). On a regional basis, some I-type granites define a trend of increasing silica content with decreasing ϵNd value (Fig. 10, Trend C1) like the isotopic variation observed in the Kangaroo Island composite dykes (Figs 7 and 10). The Kangaroo Island composite dykes (Figs 7 and 10) range from the hybridized less siliceous dacitic dyke rocks with initial ϵNd values in the range −8 to −6 to the uncontaminated S-type rhyodacite with ϵNd values of −13, which are the same as the Kanmantoo Group sediments and the Vivonne Bay–Stun Sail Boom River S-type granites. The composite dykes provide direct examples of crust–mantle interaction (Trend C1, Fig. 10b) interpreted as a major regional control on granite composition.

Significantly, the Kanmantoo Group has very different ϵNd_{500} from the Palaeoproterozoic Precambrian basement, which has Cambrian ϵNd values lower than −20, with the bulk closer to −25 (Fig. 9). No granites in the Delamerian Fold Belt have initial Nd isotopic compositions lower than those of the Kanmantoo Group. None approach the values of the more ancient basement that forms the predominant crust only 15 km to the west or NW of the Cambro-Ordovician belt. In comparison with the I–S-type granites, the post-tectonic A-types show much less crust-like isotopic compositions, with initial ϵNd values similar to Bulk Earth (−4 to +1).

Discussion

Key issues in understanding the origins of granites include the identity of their sources, the nature of the processes that modify the primary melts, and the physical causes of melting. In the Lachlan Fold Belt the initial recognition of the geochemical and mineralogical contrast between I- and S-type granite led to the concept that these granites were geochemical 'images' of specific, unique I- or S-type crustal source regions (Chappell *et al.* 1987; Chappell & White 1992). This view, however, has been countered by a number of studies (Gray 1984; Elburg 1996; Keay

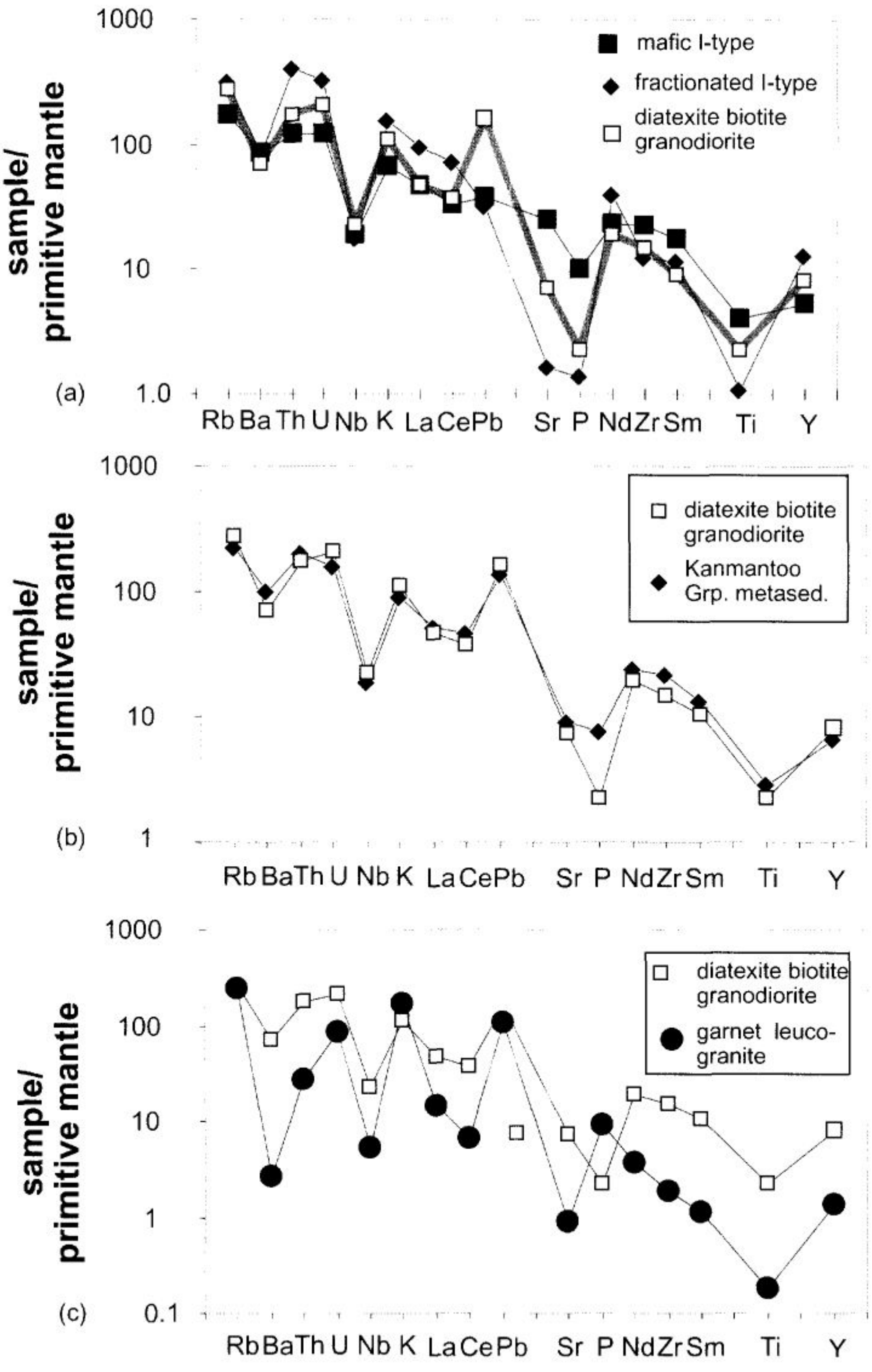

Fig. 6. Primitive mantle-normalized incompatible trace element diagrams. Normalizing values from Sun & McDonough (1989). (**a**) Comparison between a mafic, unfractionated I-type (sample GM153, Table 2, a tonalite from the Anabama intrusion), a typical I-type fractionated granite (sample 91-CYH1, Table 2) and the diatexitic S-type biotite granodiorite (VB2000-7, Table 2) from the Vivonne Bay Complex. (**b**) Comparison between the S-type biotite granodiorite (VB2000-7) and a representative example of the Kanmantoo Group metagreywackes. (**c**) Comparison between the S-type biotite granodiorite (VB2000-7) diatexite and the highly fractionated S-type garnet leucogranite from the Vivonne Bay Complex (KI-29, Table 2).

et al. 1997; Collins 1998), which (mostly with the benefit of a expanded isotopic datasets) recognize that granite genesis in the Lachlan Fold Belt involved both mantle and crustal components. Because of their many similarities, this paper develops the concept that granites have similar sources and arise by similar petrogenetic processes in both belts. A major source of debate in the Lachlan Fold Belt arises from uncertainty about the sources of the granites. By contrast, in the Delamerian belt, for reasons discussed below, we can much more confidently identify the crustal source component of the granites, and this allows us to reach some very firm conclusions about the mechanisms and settings of the production of S-type crustal melts.

Comparisons between the S- and I-type granites

The I- and S-type suites in the Delamerian belt have exactly the same general geochemical characteristics and distinctions as defined in the Lachlan Fold Belt (Chappell & White 1974, 1992). The I-type granites are relatively CaO, Ba and Sr rich. As a function of increasing silica they show depletion in FeO* (total

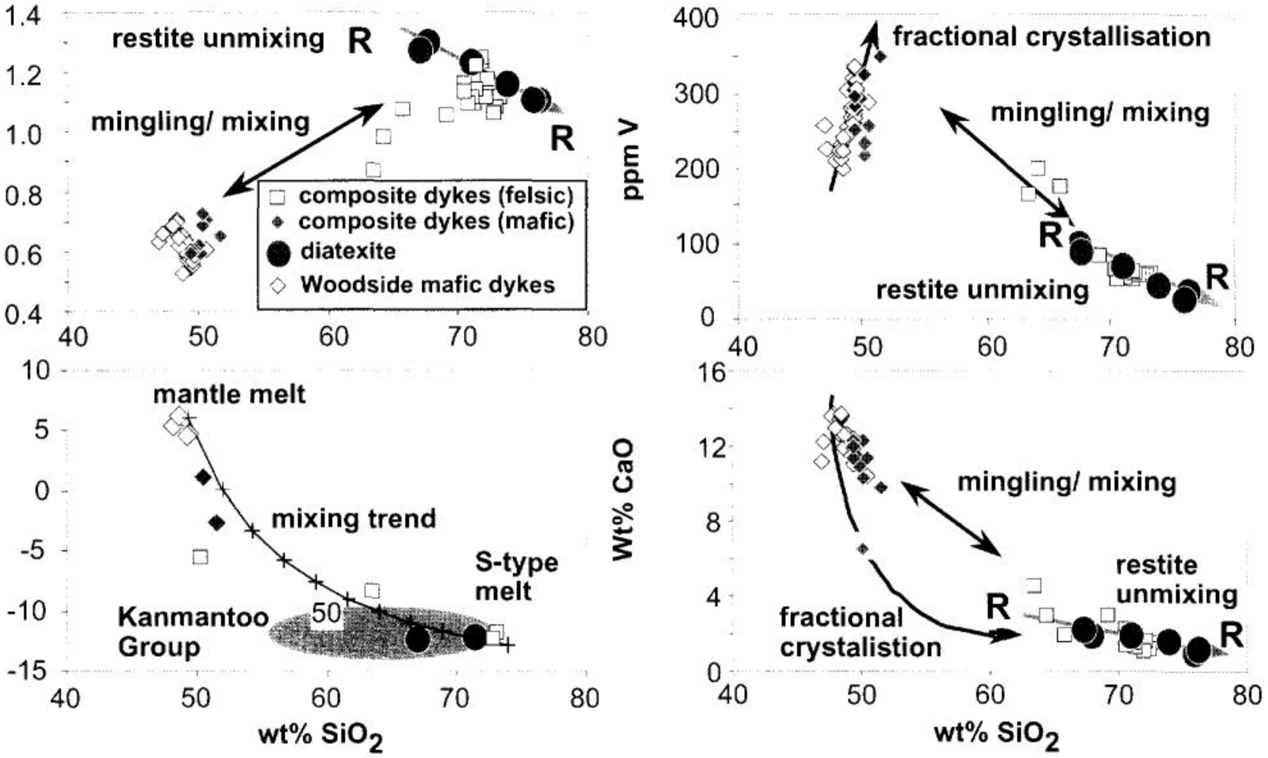

Fig. 7. Geochemical variation of ASI, V, $\epsilon Nd_{(500)}$ and CaO with silica. □, rhyodacites and dacites from the Cape Hart composite dykes; ◆, the mafic rocks from the Cape Hart composite dykes; ◇, dolerites from the similarly orientated and assumed age equivalent Woodside dyke complex (Fig. 2; Foden *et al.* 2002); shaded circles, biotite granodiorite diatexites from the Vivonne Bay–Stun Sail Boom River Complex. In the ϵNd v. SiO_2 figure the mixing trend is that produced between the garnet leucogranite S-type melt and the most primitive Woodside dolerite (Table 3). The shaded field is that of the Kanmantoo clastic sedimentary rocks.

Fe as FeO), Sc, V, Cr, Ni, Ti and P_2O_5 (Figs 4 and 5). Although at lower silica contents the I-type suites show very little variation in Mg-number, they have declining Mg-number values at higher silica levels (Fig. 4). Within the I-type suite silica enrichment is also accompanied by K_2O, Rb, Ba, Th, U and Ce enrichment.

Although the most felsic granites show geochemical continuity between the I- and S-type fields, the less siliceous S-types have rather high and constant Mg-number values and tend to have decreasing ASI with increasing SiO_2 (Figs 5, 7 and 11b (Trend R)). The I-type suites (Figs 5, 7 and 11b (Trend B)) show positive correlation between ASI and SiO_2. Like the Lachlan Fold Belt S-types (Chappell *et al.* 1987), and best illustrated by the Kangaroo Island diatexites (Figs 7 and 11a), the most mafic S-type granites have the highest ASI values as well as the highest V and MgO. These also have the highest Pb, Y and REE (Fig. 4). In comparison with the I-types, the S-types are also more Na_2O and CaO poor at given silica levels (Figs 4 and 5) and are marginally more MgO and P_2O_5 rich. More fractionated (low Mg-number) I-types tend to have lower Sr and P than siliceous S-types.

The S-types (defined to have ASI values > 1.1) all have initial ϵNd values of < -7.5 and initial $^{87}Sr/^{86}Sr$ values mostly > 0.714. The I- and A-types all have $\epsilon Nd > -7.5$ and initial $^{87}Sr/^{86}Sr < 0.714$ (Table 4, Fig. 9). Geochemically, the I-type series falls between the fields of mafic rocks and of felsic true granites (Figs 4, 5 and 11). As demonstrated by Nd-isotopic v. Mg-number or SiO_2 variation (Fig. 10; Trends A and B), the felsic endpoint of this trend ranges from S-type granite with local crustal isotopic compositions to very fractionated A-type granite with more primitive Nd isotopic ratios. The trend towards local crust is one of increasing $^{87}Sr/^{86}Sr$ and decreasing $^{143}Nd/^{144}Nd$ (Trend B, Fig. 9).

We regard the field of S-type granites as bracketed by three limiting evolutionary trends. Two of these incorporate isotopic variability with declining initial $^{87}Sr/^{86}Sr$ and increasing initial $^{143}Nd/^{144}Nd$ (Trend C, Fig. 9). Of these two trends one shows continuity with the I- to A-type granitoid suites (Trend C1, Fig. 10b) and the other is towards mafic magmas (Trend C2, Fig. 10b, compare Kangaroo Island composite dykes). The third S-type granite trend (Trend R in Figs 7, 8 and 11) is one with a constant initial ϵNd value (-13.5 ± 0.5) and is typified by the diatexites from Kangaroo Island. This trend is towards lower silica and high Mg-number and ASI values (Figs 4 and 11), and diverges from the I–S granites in having higher Pb, Ni, and P_2O_5.

Source and origin of the S-type granites

Source of the S-type granites. The Kangaroo Island outcrops reveal four distinct types of S-type melt behaviour: (1) formation by partial melting of the Kanmantoo Group metasediments under restite–melt control (diatexite); (2) mingling of the S-type diatexite with intrusive more I-type granite magma; (3) segregation and fractional crystallization of S-type melts to produce leucogranites; (4) mingling and hybridization of S-type melts with intruding basaltic melts.

The outcrops at Vivonne Bay and Stun Sail Boom River provide direct evidence for the local production of S-type granite

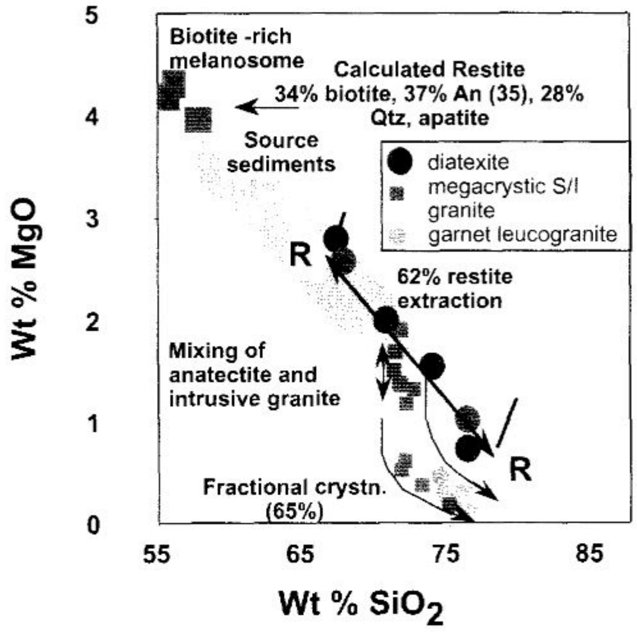

Fig. 8. MgO v. SiO_2 variation illustrating the relationships between the Kangaroo Island S-type complexes. Shaded envelope: local composition of Kanmantoo Group sedimentary rocks (psammo-pelites greywackes); large shaded circles, biotite granodiorite diatexite from Vivonne Bay and Stun Sail Boom River; shaded squares, the intrusive, porphyritic granite at Vivonne Bay and Stun Sail Boom River; small shaded circles, garnet leucogranite; crossed squares, biotite melanosome rocks from Vivonne Bay. The 62% restite trend shown illustrates the extent of variation resulting from extraction of 62% of a restite composed of biotite (35%) + An_{35} plagioclase (37%) + quartz (28%) + minor apatite (Table 6). Large shaded square, bulk composition of this restite. R R is the restite-controlled diatexite trend.

melts (diatexite) from the Kanmantoo Group metasedimentary rocks (Fig. 3). These granites have the same Nd Sr isotopic composition (initial εNd = −13 ± 0.5) as the metasediments from which the field relations indicate they were derived, with slightly lower Mg-number or higher SiO_2 as anticipated as a result of partial melting (Figs 7 and 8). The normalized incompatible element pattern of the diatextite is also the same as that of the Kanmantoo sediment, distinguished from the other granites by having a significant positive Pb anomaly (Fig. 6). Thus the combination of field, geochemical and isotopic evidence points strongly to the Kanmantoo Group as the S-type endmember in at least the southern Delamerian Fold Belt. At its more felsic end, the biotite granodiorite–granite diatexite series has compositions the same as the rhyodacite magmas from the composite dykes (Figs 7 and 11) and like the transitionally I S-type intrusive megacrystic granite. This similarity suggests that the rhyodacite dyke magmas and the megacrystic intrusive granite also originated from the same type of source as the diatexite, reflecting similar processes of melt production and segregation.

It is surprising that although the Kanmantoo basin is formed by faulting of the well-characterized pre-Adelaidean Palaeoproterozoic cratonic basement rocks (Fig. 2), the latter do not contribute to the crustal melt components identifiable in the Cambro-Ordovician S-type granites (Fig. 9). This conclusion is also supported by the observation that inherited zircon in Delamerian I-type granite (Foden *et al.* 1999) was not from the Meso- to Palaeoproterozoic basement but had age frequency population patterns identical to the very distinctive patterns of the Kanmantoo Group (Ireland *et al.* 1998).

It appears that the role of the Kanmantoo Group in the Delamerian Orogen was like that of the Ordovician flysch as the major source of the S-type granites in the Lachlan Fold Belt (Collins 1998; Keay *et al.* 1997). We note that in the Lachlan Fold Belt, although earlier interpretations had considered the Ordovician flysch as a geochemically inappropriate source for the Lachlan Fold Belt S-type granites (Chappell 1996), recent zircon age frequency data indicate that the inherited zircon populations in both I- and S-type granites are indistinguishable from those that could be derived from this source (Williams *et al.* 1992). The combination of Nd Sr isotopic data and field and geochemical arguments has led recent workers (Collins 1998; Keay *et al.* 1997) to support the model put forward by Gray (1984), that the Lachlan Fold Belt S-type endmember is indeed a partial melt of the Ordovician flysch. These models have been developed and tested at Cooma in NSW (Fig. 1), where the Cooma Granodiorite is undisputedly derived by partial melting of the Ordovician flysch (Collins & Hobbs 2001) and where processes and geological relations are like those we describe at Vivonne Bay–Stun Sail Boom River from Kangaroo Island.

Petrogenesis of the S-type granites. Our results establish the Kanmantoo Group as the S-type granite source and, as discussed above, we postulate that intra-suite geochemical variation is controlled both by mixing or mingling with I-type and mafic magmas (Trend C in Figs 9–11) and by variable melt–residue unmixing (Trend R in Figs 7, 8 and 11). This melt–residue (restite) unmixing trend is best illustrated by the diatexites from Kangaroo Island. Least-squares mixing calculations model this trend (Figs 7 and 8) as one controlled by the assemblage quartz–biotite (Mg-number 0.75)–plagioclase (An_{17})–apatite. As summarized by the MgO SiO_2 relationships (Fig. 8), the range in compositions covered by the granite–granodiorite diatexite series represents about 45% restite extraction. The bulk composition of the calculated restite also matches that of the biotite melanosome rocks (Figs 8 and 11). These relationships imply that generation of S-type granite magmas is controlled by a near-isothermal melt production and segregation from metasedimentary migmatite complexes (restite control).

At Vivonne Bay there are also garnet leucogranites with marked depletions of trace elements such as Sr, Zr and Ti, which indicate they have evolved by melt segregation and fractional crystallization. Least-squares mixing calculations (Table 6) indicate control by quartz–plagioclase (*c.* An_{12})–biotite fractionation. This assemblage differs from the restite calculated previously in having less An-rich plagioclase and a larger proportion of quartz relative to biotite and plagioclase. For a range of trace elements the *D* values required to yield the observed concentrations in the garnet leucogranite, based on the crystallization proportion calculated in the least-squares calculation, were estimated (Table 6). These indicate that most elements, including the REE, are highly compatible, confirming the involvement of accessory phase saturation (zircon, monazite, apatite).

In addition to the restite-dominated processes, we have also noted that some Delamerian S-type granite compositions are displaced towards the I-type field. This trend is probably one of contamination. It tends towards higher Nd- and lower Sr-isotopic ratios. Because it is improbable that a near minimum temperature S-type melt will assimilate any solid basalt, this contamination

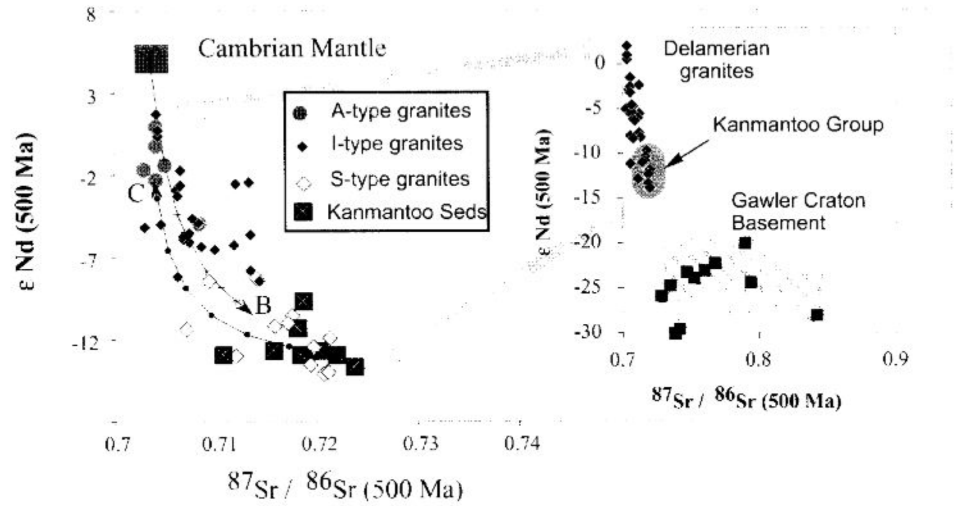

Fig. 9. $\epsilon Nd_{(500)}$ v. $^{87}Sr/^{86}Sr_{(500)}$ variation of the various sub-groups of the Delamerian granites. Symbols as indicated. Trend B is calculated AFC trend (formulation of Powell 1984) modelling the contamination and progressive crystallization of a Cambrian basaltic parent magma by Kanmantoo Group metasediment (parent basalt: Nd 5 ppm, $\epsilon Nd_{(500)}$ −5, Sr 200 ppm, $^{87}Sr/^{86}Sr$ 0.7035; crustal contaminant: Nd 30 ppm, $\epsilon Nd_{(500)}$ −13, Sr 180 ppm, $^{87}Sr/^{86}Sr$ 0.7220; bulk distribution coefficients: D_{Nd} = 0.5, D_{Sr} = 0.8). Tick marks indicate 10% crystallization intervals. r = 0.45 (assimilation rate/crystallization rate). Trend C is direct mixing trend between a crustal partial melt of Kanmantoo Group metasediment with a composition of the Vivonne Bay garnet leucogranite and Cambrian basalt. It should be noted that this is the same model as illustrated in Fig. 7. Inset: $\epsilon Nd_{(500)}$ v. $^{87}Sr/^{86}Sr_{(500)}$ variation of the combined Delamerian granites. The diagonally striped envelope is range of available unpublished data (45 samples) from Gawler Craton basement granite gneiss, granite, felsic and intermediate volcanic rocks and metasedimentary samples (■, data points from Turner *et al.* 1993b).

of the crustal melts was probably the result of mingling and hybridization caused by magma mixing. The process of direct mixing is clearly illustrated by the observed hybridism in the composite dykes and yields a modelled close match of Sr–Nd isotopic trends (Trend C, Fig. 9), and of isotope–major element covariation (see ϵNd v. SiO_2, Figs 7 and 10). This hybridism can result by mixing either with mafic magmas (as in the case of the Cape Hart composite dykes; Figs 7 and 11) or, as indicated by field relations at Vivonne Bay, with granite intrusions of more I-type composition.

We note that the Lachlan Fold Belt S-type granites also show trends like those of the Kangaroo Island diatexites. This trend of increasing ASI with decreasing silica (Trend R, Fig. 11) has sometimes been used to deny the role of mixing between mantle and peraluminous crustal melts, suggesting such a trend would require a more peraluminous mafic endmember (Chappell *et al.* 1987). Our data clearly highlight that this is a restite accumulation trend associated with the generation of crustal melts and is separate from, but might coexist with, mafic mingling trends towards lower ASI (Trend C, Fig. 11).

Source and origin of the I-type granites

Trends of variation of ϵNd v. Mg-number or silica content (Fig. 10) highlight two extremes in evolutionary path originating at the mafic or low-silica end of the I-type series. One of these leads to the younger, largely post-tectonic A-type granites (Foden *et al.* 1999) and the other to the syntectonic S-type granites (Fig. 10). The trend to the A-type field is towards very low-Mg-number, silica- and incompatible element-enriched granites (Figs 4, 10) whose Nd and Sr isotopic compositions are only slightly shifted from those of the mafic magmas (Fig. 9). These trends are produced dominantly by fractional crystallization (Turner *et al.* 1992; Turner & Foden 1996), apparently with only limited crustal assimilation. The second trend links the I-type granites to the field of the S-type granites and of the Kanmantoo sediments. This is defined by marked decrease in ϵNd and by lesser decline in Mg-number (Figs 4, 9 and 10a). Given their convergence with the S-type granite field, these trends indicate that the I-type granites evolved from the assimilation of Kanmantoo-type crustal rocks either by contemporary cooling and fractionating mafic magmas, or by mixing of these mafic magmas with the S-type granite magmas derived from these sediments. At its mafic end, the I-type granite field is in direct geochemical and isotopic continuity with the Cambrian mafic rocks.

Because all the I-type granites have initial ϵNd values greater than those of any known basement rock sequences, the Nd isotope data require direct involvement of mantle melts in the production of the Delamerian I-type granite magmas. It is also clear from the inflected, curvilinear geochemical trends of the I-type granites that fractional crystallization processes must also be involved. In particular, the transition from mafic tonalite to siliceous granodiorite is one of initial enrichment of P, Sr, LREE, Zr and Pb, later followed by depletion (Figs 4 and 5). These trends are explained as the result of fractional crystallization, consistent with changing K_d values as progressive (particularly accessory) phase saturation took place during falling temperatures. Minerals precipitated during the middle to late stages of cooling are K-feldspar, zircon, apatite, titanite and allanite. These inflected trends cannot be explained by simple mixing of felsic crustal melts with mafic magmas as occurs in the Kangaroo Island composite dykes. Thus our evidence supports the combined roles of both fractional crystallization and assimilation, favouring the evolution of the I-type suites by an AFC process

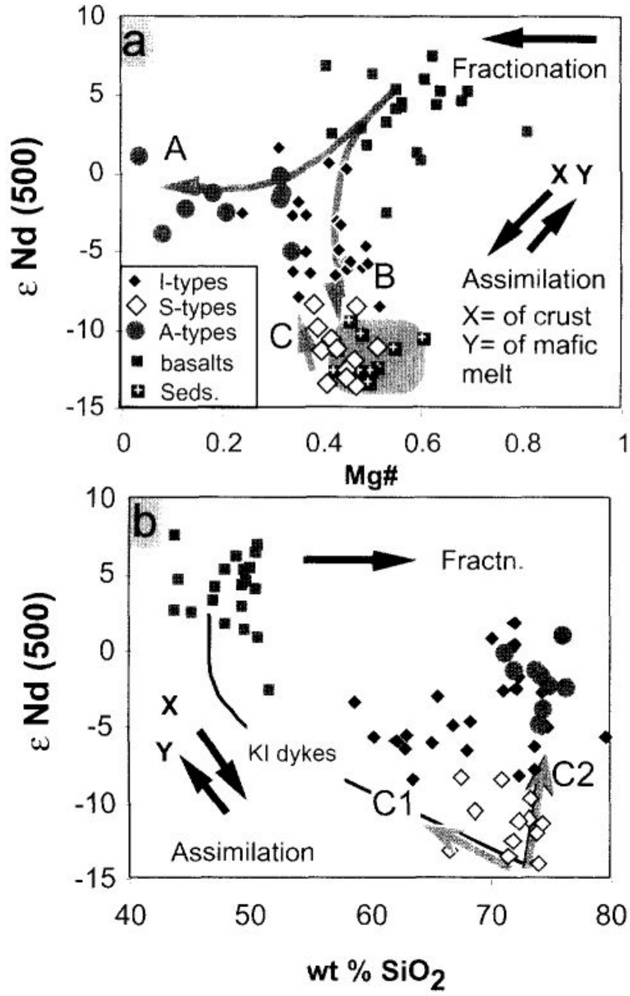

Fig. 10. (**a**) $\epsilon Nd_{(500)}$ v. Mg-number variation of the various sub-groups of the Delamerian granites from the entire belt in South Australia and Victoria. Shaded squares with crosses and shaded field, Kanmantoo Group sediments; , S-type granites; ◆, I-type granites; ○, post-tectonic A-type granites; ■, Cambrian basalts. Data for the A-type granites from Turner *et al.* (1992) and Turner & Foden (1996). Trend A is fractionation-dominant trend from basaltic parent melt and leading to the A-type granites (low assimilation trend). Trend B is high assimilation and fractionation trend commencing from basaltic parent melt and leading to the I-type granites. Trend C is crustal partial melt (of Kanmantoo Group), contaminated by mixing with either basalt or I-type granite. (**b**) $\epsilon Nd_{(500)}$ v. wt% SiO_2. Symbols as in (**a**). Trend C1 is crustal melt mixing with basaltic contaminant. Trend C2 iscrustal melt mixing with I-type granite contaminant. Trend of Kangaroo Island composite dykes indicated.

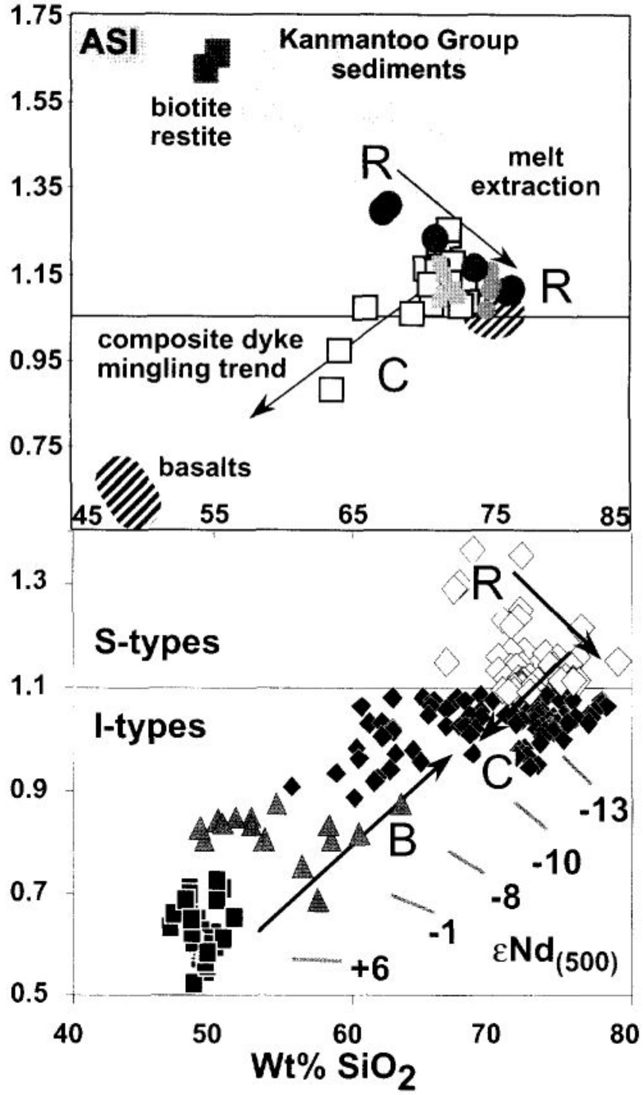

Fig. 11. (**a**) ASI v. SiO_2 variation showing the Kangaroo Island S-type complexes and the composite dykes. Symbols as in Figs 7 and 8. Striped field, Cape Willoughby granite; 'basalts' is the field of dolerite dyke rocks from Cape Hart and Woodside. Trend R–R is the restite–S-type melt (diatexite) unmixing trend (as in Figs 7 and 8). Trend C (as in Figs 9 and 10) is the trend of mafic contamination of the felsic dyke rocks. (**b**) Regional ASI v. SiO_2 variation (symbols as in Fig. 4) also summarizing Nd-isotope variation in I type granite. Trend B (as in Figs 9 and 10) is the AFC dominant trend producing I-type granites; Trend C (as above) is the mixing trend with I-type or mantle melts displacing S-type (crustal melt) compositions towards higher ϵNd values; Trend R is the restite–diatexite trend (as above and in Figs 7 and 8) showing extraction of S-type melts from their sources.

(DePaolo *et al.* 1992). This process started with basaltic magmas (Table 3) of E-MORB affinities (Foden *et al.* 2002) whose compositions evolved towards felsic compositions as a result of crystallization and contamination leading to siliceous I-type granites. These resultant felsic magmas are more depleted in Ni, V, Cr and Sc than the S-type granites.

AFC trends of Nd- v. Sr-isotopic variation (Fig. 9, Trend B) were calculated using the equations of DePaolo (1981) and Powell (1984). The I-type trend was modelled using the Sr and Nd concentrations and isotopic compositions of the most primitive Delamerian basalt as the mantle endmember (Table 3), and the mean composition of the Kanmantoo Group as the crustal endmember. The D values used for both Nd and Sr were < 1, mimicking the crystallization of an assemblage dominated by moderately Ca-rich plagioclase, hornblende and clinopyroxene. The AFC equation contains a parameter r, which is the ratio of

Table 5. *Isotope composition of mineral separates: Stun Sail Boom River; Rb–Sr isochron*

Sample: Phase:	5511 Apatite	5511 Muscovite	5511 Biotite	5516 Apatite
$^{87}Sr/^{86}Sr$	0.721117	0.820852	2.189730	0.721613
± 1 SD	0.000059	0.000086	0.000119	0.000072
Rb (ppm)	5.48	385.99	677.72	3.52
± 1 SD	0.234	0.419	0.382	0.066
Sr (ppm)	218.64	77.90	10.64	147.51
± 1 SD	0.053	0.022	0.003	0.028
$^{87}Rb/^{86}Sr$	0.07	14.49	210.91	0.07
% SD Rb/Sr	1	1	1	1
$^{143}Nd/^{144}Nd$1	0.512122	**SS11 (Rb–Sr isochron)**		0.512067
± 1 SD	0.000052	**Age = 487.4 ± 3.5 Ma**		0.000030
Nd (ppm)	570.26	**Initial ratio = 0.72062**		618.66
Sm (ppm)	227.09	**MSWD = 0.25**		227.56
$^{147}Sm/^{144}Nd$	0.2407			0.2223
$\epsilon T = 0$	−10.1			−11.1
ϵ@500 Ma	−12.9			−12.8

$^{87}Sr/^{86}Sr$ SRM 987 is 0.71028474 ± 0.000043; $^{143}Nd/^{144}Nd$ La Jolla is 0.51157285 ± 0.000021. Corrected to La Jolla $^{143}Nd/^{144}Nd$ 0.5116240.

the rate of assimilation to the rate of crystallization. Curve B in Fig. 9 was determined using a high r value (0.45). With these parameters the resultant hybrid melt reached ϵNd −7 after about 50% crystallization. If a much smaller r value were to be used the curve would only reach the field of post-tectonic A-type granites with *c.* ϵNd −2 after 60% crystallization.

Although, in explaining the Lachlan Fold Belt granites, Keay *et al.* (1997) and Collins (1998) doubted the role of AFC and to a large extent emphasized mixing, the Delamerian ϵNd v. Mg-number and ϵNd v. wt% SiO_2 (Fig. 10) trends highlight the vital role of this process. The model we propose for the Delamerian granites is similar to those used in earlier studies to explain the composition of many Cenozoic volcanic and intrusive rocks in the western North and South America (Hildreth 1981; Farmer & DePaolo 1983, 1984; Hildreth & Moorbath 1988; DePaolo *et al.* 1992). Those studies emphasized the interactive role of contemporary mantle-derived mafic magmas with isotopically distinctive continental crust. Likewise, exposures of very deep crustal mafic magma chamber sequences from the Ivrea Zone (Voshage *et al.* 1990) in the Alps provide direct support of the role of processes of interaction between mantle melts and the crust, closely mirroring those modelled by Sparks *et al.* (1984) and Huppert & Sparks (1988).

Whereas Farmer & DePaolo (1984) attempted to model the extent to which crust v. mantle contributions to granitic magmas varied as a function of crustal thickness and rate of basalt magma flux alone, DePaolo *et al.* (1992) emphasized that the relative extent of these two contributions is more dependent on the thermal state of the wall rocks. High wall-rock temperatures will result in high assimilation rates. If this reasoning is applied to the granites in the Adelaide Fold Belt, we must conclude that the earlier synconvergent granites have been generated at sites where crustal wall rocks were hotter than the much less contaminated post-convergent A-type granites.

We propose that at the onset of the Delamerian Orogeny, crustal deformation was focused, partly by thermal weakening (Sandiford *et al.* 1992; Stüwe *et al.* 1993), at the Kanmantoo basin. This led to crustal thickening and the stalling of rising dense, mantle-derived mafic melts near the Moho. The AFC processes we have documented are the consequence of the thermal and geochemical interaction between stalled mafic intrusions and continental crust (Kanmantoo basin fill). High crustal temperatures resulted in high assimilation rates (high r values) yielding I–S type granites. The S-types are byproducts of this process, being melts of the wall rocks adjacent to the cooling mafic to I-type magma bodies. Post-convergent extension then allowed the mafic melts to rise higher in the crust (as illustrated by the Kangaroo Island composite dykes) as a result of crustal thinning and dilatant fracturing. These mafic magmas may then have ponded at shallow depths and fractionated without crustal assimilation, yielding the A-type granites (low r values). This trend of diminishing crustal component at the late orogenic stage is like that reported in the caldera-forming rhyolites of mid- to late Cenozoic age of the western USA (Perry *et al.* 1992) formed during Basin and Range extension.

Granite magmatism in a periodically extended convergent plate margin

The Kanmantoo Group sediments were rapidly deposited in a deep, narrow basin (inset, Fig. 2). Basin formation was associated with extension and decompressional mantle melting. As a result, the Kanmantoo sediments were intruded by Early Cambrian mafic magmas (Table 3). The onset of deformation brought an immediate transition to granite magmatism ranging from I- to S-type. During the syntectonic phase, when Delamerian crustal thickening was maximal, mafic magmas were stalled in the lower crust and underwent hybridization. In the subsequent post-tectonic extensional phase (Oliver & Zakowski 1995) these mafic melts rose much closer to the surface and cooled and fractionated in contact with cold upper-crustal rocks, experiencing only limited crustal contamination.

The cycle of events on Kangaroo Island highlights the close interrelationship between evolving strain and magmatic histories. The earliest (509 ± 7 Ma) granite is the fractionated S-type at Cape Willoughby, where field relations imply this is a deformed sill that intruded layer parallel to the host Kanmantoo Group metasediments. This granite intruded early in the Delamerian orogenic history as a result of mantle heating of the Kanmantoo sedimentary pile. The sill-like form of the intrusion implies that the minimum compressive stress (σ_3) was vertical (lithostatic), and that the NNW-directed tectonic driving force (σ_1) was just developing. The Vivonne Bay–Stun Sail Boom River suites (504 ± 8 Ma) were syntectonic crustal melts formed *in situ* as a result of advective heat transfer by the plutonic I–S granites. These in turn must have formed by basalt–Kanmantoo Group

Table 6. *Least-squares mixing models*

	Least squares model for diatexitic granite						
	Granodiorite	Granite	Modelled granite			%	Restite
	VB2000-5	ME-378					
SiO_2	67.76	76.00	76.06		Biotite	21.50	34.65
TiO_2	0.64	0.29	0.29		Plagioclase (An_{35})	22.90	36.91
Al_2O_3	14.32	12.00	12.06		Apatite	0.15	0.24
FeO	4.90	1.96	1.91		Quartz	17.50	28.20
MnO	0.07	0.03	0.03	A	**% Crystals**	**62.05**	
MgO	2.66	0.76	0.73	+			
CaO	2.04	1.03	0.84	B	**% Liquid =**		
Na_2O	2.12	2.17	1.85		**Granite**	**37.95**	
K_2O	3.50	4.94	4.31	=			
P_2O_5	0.12	0.10	0.16	C	Biotite granodiorite	1.00	
					Sum of res.^{2}	0.545	

	Least squares model for garnet leucogranite						
	Granite Ki-07	Leucogranite Ki-29	Modelled leucogranite			%	Restite
					Biotite	14.90	29.30
SiO_2	71.88	76.55	76.62		Plagioclase (An_{12})	17.20	33.90
TiO_2	0.51	0.04	0.04		Apatite	0.40	0.70
Al_2O_3	13.59	13.61	13.6		Quartz	18.30	36.00
FeO	2.9	0.33	0.34	A	**% crystals**	**50.8**	
MnO	0.05	0.01	0.01	+			
MgO	1.34	0.19	0.19	B	**% Liquid =**		
CaO	1.66	0.55	0.47		**Garnet granite**	**49.7**	
Na_2O	2.77	2.81	2.79	=			
K_2O	4.04	5.13	5.05	C	Porphyritic granite	100	
P_2O_5	0.23	0.2	0.2		Sum of res.^{2}	0.018	

Calculated bulk distribution coefficients (*D*) in generation of garnet leucogranite (model 2 above)

Element	*D*
Rb	1.4
Sr	3.9
Ba	5.7
Zr	3.95
Nb	3
Nd	3.06
Sm	2.95
Y	2.8
Sc	3.3

Restite indicates calculated mineral assemblage normalized to 100% melt-free.

metasediment interaction at greater depth. Finally the composite dykes (500 ± 7 Ma) mark the weakening of the main tectonic stress (σ_1), and the development of roughly east–west extension (σ_3 now horizontal). Importantly, the composite dykes indicate that S-type magma chambers are established deeper in the metasedimentary tectonic pile as a result of crustal melting, but also that these have then been invaded by mantle-derived mafic melts. The mafic melts provide clear evidence of the heat source for crustal melting. Their transport in dykes to shallower crustal levels not previously invaded by mafic melts must be a response to the transition to extension and crustal thinning. Our Rb–Sr date of 487 ± 3 Ma (Table 5) is the same as the magmatic age of the post-tectonic A-type granites and represents the age of exhumation and cooling of the terrane. This uplift event is also observed elsewhere in the Delamerian belt at the same time, including Tasmania (Raheim & Compston 1977) and created the erosive highland source of the Lachlan Fold Belt flysch blanket (Turner *et al.* 1996).

We conclude that pre-convergent rifting played a vital role in the subsequent geological and magmatic evolution of the Delamerian Belt and that the S-type granite source was provided by recently introduced basin fill in a deep, localized trough. This basin fill melted in preference to the older crustal walls of the basin probably because of its water content and fertility. The evolution of the Delamerian belt from Kanmantoo Group deposition through convergent deformation to terminal uplift and post-tectonic extension lasted a total of 40 Ma (525–485 Ma), marking a cycle of oscillation from extension to compression and back to extension.

The cycle of rapid transitions from extension to compression and back to extension in the Delamerian belt continued to be a feature of the tectonic evolution of eastern Australia through Phanerozoic time, particularly during the Palaeozoic evolution of the Lachlan Fold Belt (Gray 1997). There, examples of specific localized extensional (or transtensional) sedimentary basins with geological histories very like that of the Kanmantoo basin include the Melbourne–Mansfield Trough (O'Halloran & Cas 1995), the Eden Yalwal Trough (Fergusson *et al.* 1979) and the Mathinna trough in northeastern and western Tasmania (Burrett & Martin 1989) (Fig. 2). There are examples of linear belts of metamorphic complexes whose thermotectonic history is also very like that of the Kanmantoo. (e.g. the Late Ordovician–Early Silurian Bradley's Creek–Cooma Complex–Kuark Complex belt (Carson & Rickard 1998)). It may be that granite magmatism in the Lachlan Fold Belt, as in the Delamerian belt, is a reflection of deep, narrow rifts, buried under a widely distributed flysch blanket.

Summary and conclusions

In the South Australian sector of the Cambro-Ordovician Ross–Delamerian Orogen granite production is largely confined to deep, Early Cambrian, sediment-filled basins where granites are associated with mafic rocks. The syntectonic suites have compositions forming a continuum between I- and S-types. After the cessation of convergent deformation at *c.* 490 Ma an abrupt transition to a bimodal magmatic association of mafic intrusions and felsic granites and volcanic rocks of S- and A-type affinities occurred.

The formation of S-type magma is well illustrated by exposed migmatite complexes on the south coast of Kangaroo Island. These magmas originated as *in situ* partial melts of the Early Cambrian sediments where these were intruded by either mafic or I–S granite magmas. These migmatite complexes were mingled with the intrusive magmas that provided the heat sources for crustal melting. Our data indicate that S-type magma production and migration is controlled by variable segregation of restite and melt. The direct role of mantle-derived melts in the process of crustal partial melting is indicated by composite S-type rhyodacite–dolerite dykes.

The syntectonic to early post-tectonic I-type granite magmas resulted from the assimilation of crustal melts by intruding mafic magmas. This process was coupled with fractional crystallization (AFC). This stage of magma production occurred when high lower-crustal temperatures were developed during the later stages of convergent deformation, resulting in high crustal assimilation rates. The A-type granites cluster towards the mantle endmember. These were formed when post-convergent extension allowed mafic melts to rise and pond at shallow depths and fractionate without crustal assimilation.

We are grateful to technical staff in the Department of Geology and Geophysics at Adelaide University. In particular, we thank D. Bruce for his assistance in the isotope laboratory and J. Stanley for XRF data. M.E. acknowledges the support of an ARC post-doctoral fellowship. The paper was significantly improved by constructive reviews by R. Maas and C. Barnes.

References

Bea, F., Fershtater, G. & Corretgé, L.G. 1992. The geochemistry of phosphorus in granite rocks and the effect of aluminium. *Lithos*, **29**, 43–56.

Burrett, C.F. & Martin, E.L. 1989. *Geology and Mineral Resources of Tasmania*. Geological Society of Australia, Special Publication, **15**.

Carson, L.J. & Rickard, M.J. 1998. Early recumbent fold hinge in the Bradley's Creek Metamorphic Complex, near Canberra, Australia. *Australian Journal of Earth Sciences*, **45**, 501–508.

Cas, R.A. 1983. *A Review of the Palaeogeographic and Tectonic Development of the Palaeozoic Lachlan Fold Belt of Southeastern Australia*. Geological Society of Australia, Special Publication, **10**.

Chappell, B.W. 1996. Magma mixing and the production of compositional variation within granite suites: evidence from the granites of southeastern Australia. *Journal of Petrology*, **37**, 449–470.

Chappell, B.W. & White, A.J.R. 1974. Two contrasting granite types. *Pacific Geology*, **8**, 173–174.

Chappell, B.W. & White, A.J.R. 1992. I- and S-type granites in the Lachlan Fold Belt. *Transactions of the Royal Society of Edinburgh: Earth Sciences*, **83**, 1–26.

Chappell, B.W., White, A.J.R. & Wyborn, D. 1987. The importance of residual source material (restite) in granite petrogenesis. *Journal of Petrology*, **28**, 1111–1138.

Collins, W.J. 1998. Evaluation of petrogenetic models for Lachlan Fold Belt granitoids: implications for crustal architecture and tectonic models. *Australian Journal of Earth Sciences*, **45**, 483–500.

Collins, W.J. & Hobbs, B.E. 2001. What caused the Early Silurian change from mafic to silicic (S-type) magmatism in the eastern Lachlan Fold Belt? *Australian Journal of Earth Sciences*, **48**, 25–41.

Coney, P.J., Edwards, A., Hine, R., Morrison, F. & Windrim, D. 1990. The regional tectonics of the Tasman orogenic system, eastern Australia. *Journal of Structural Geology*, **12**, 519–544.

Cooper, J.A., Jenkins, R.J., Compston, W. & Williams, I.S. 1992. Ion-probe zircon dating of a mid-Early Cambrian tuff in South Australia. *Journal of the Geological Society, London*, **149**, 185–192.

Dalziel, I.D. 1991. Pacific margins of Laurentia and East Antarctica–Australia as a conjugate rift pair: evidence and implications for an Eocambrian supercontinent. *Geology*, **19**, 598–601.

DePaolo, D.J. 1981. Trace element and isotopic effects of combined wallrock assimilation and fractional crystallization. *Earth and Planetary Science Letters*, **53**, 189–202.

DePaolo, D.J., Perry, F.V. & Baldridge, W.S. 1992. Crustal versus mantle sources of granite magmas: a two-parameter model based on Nd isotopic studies. *Transactions of the Royal Society of Edinburgh: Earth Sciences*, **83**, 439–446.

Dymoke, P. & Sandiford, M. 1992. Phase relationships in Buchan Facies Series pelitic assemblages: calculations with applications to andalusite–staurolite parageneses in the Mount Lofty Ranges, South Australia. *Contributions to Mineralogy and Petrology*, **110**, 121–132.

Elburg, M.A. 1996. Evidence of isotopic equilibration between microgranitoid enclaves and host granodiorite, Warburton Granodiorite, Lachlan Fold Belt, Australia. *Lithos*, **38**, 1–22.

Elburg, M.A. & Nicholls, I.A. 1995. The origin of microgranitoid enclaves in the S-type Wilson's Promontory Batholith, Victoria: evidence for magma mingling. *Australian Journal of Earth Sciences*, **42**, 423–435.

Fanning, C.M. 1990. *Single grain dating of a granite sample from Cape Willoughby, Kangaroo Island*. Prise Laboratories, Australian National University Progress Report 89-060. S.A. Department of Mines and Energy, Open File Envelope **8828**, 29–32.

Farmer, G.L. & DePaolo, D.J. 1983. Origin of Mesozoic and Tertiary granite in the western United States and implications for pre-Mesozoic crustal structure: I. Nd and Sr isotopic studies in the geocline of the northern Great Basin. *Journal of Geophysical Research*, **88**, 3379–3401.

Farmer, G.L. & DePaolo, D.J. 1984. Origin of Mesozoic and Tertiary granite in the western United States and implications for pre-Mesozoic crustal structure: II. Nd and Sr isotopic studies of Cu- and Mo-mineralized granite in the Precambrian craton. *Journal of Geophysical Research*, **89**, 141–160.

Fergusson, C.L., Cas, R.A., Collins, W.J. & 5 others 1979. The Upper Devonian Boyd Volcanic Complex, Eden, New South Wales. *Journal of the Geological Society of Australia*, **26**, 87–106.

Fergusson, C.L., Cas, R. & Stewart, I.R. 1989. Ordovician turbidites of the Hotham Group, eastern Victoria: sedimentation in deep-marine channel–levee complexes. *Australian Journal of Earth Sciences*, **36**, 1–12.

Fleming, P.D. & White, A.J.R. 1984. Relationships between deformation and partial melting in the Palmer migmatites, South Australia. *Australian Journal of Earth Sciences*, **31**, 352–360.

Flöttmann, T., Haines, P., Jago, J., James, P., Belperio, A. & Gum, J. 1998. Formation and reactivation of the Cambrian Kanmantoo Trough, SE Australia: implications for Early Palaeozoic tectonics at eastern Gondwana's plate margin. *Journal of the Geological Society, London*, **155**, 101–115.

Flöttmann, T., James, P., Menpes, R. & 5 others 1995. Kangaroo Island, South Australia: strain and kinematic partitioning during Delamerian basin and platform reactivation. *Australian Journal of Earth Sciences*, **42**, 35–49.

Flöttmann, T., James, P., Rogers, J. & Johnson, T. 1994. Early Palaeozoic foreland thrusting and basin reactivation at the Palaeo-Pacific margin of the southeastern Australian Precambrian Craton: a reappraisal of the structural evolution of the southern Adelaide Fold–thrust Belt. *Tectonophysics*, **234**, 95–116.

Foden, J., Sandiford, M., Dougherty-Page, J. & Williams, I. 1999. Geochemistry and geochronology of the Rathjen Gneiss: implications for the early tectonic evolution of the Delamerian Orogen. *Australian Journal of Earth Sciences*, **46**, 377–389.

Foden, J., Song, S.-H., Turner, S.P., Elburg, M.A., Smith, P., Van der Steldt, B. & Van Penglis, D. 2002. Geochemical evolution of the lithospheric mantle beneath S.E. South Australia. *Chemical Geology*, **182**, 663–695.

Foden, J.D., Turner, S.P. & Morrison, R. 1990. The tectonic implications of the Delamerian magmatism in South Australia and western Victoria. *In:* Jago, J.B. & Moore, P.S. (eds) *The Evolution of a Late Precambrian Early Palaeozoic Rift Complex: the Adelaide Geosyncline*. Geological Society of Australia, Special Publication, **16**, 483–495.

Gibson, G.M. & Nihill, D.N. 1992. Glenelg River Complex: western margin of the Lachlan Fold Belt or extension of the Delamerian Orogen into Western Victoria? *Tectonophysics*, **214**, 69–91.

Gray, C.M. 1984. An isotopic mixing model for the origin of granitic rocks in southeastern Australia. *Earth and Planetary Science Letters*, **70**, 47–60.

Gray, D. 1997. Tectonics of the southeastern Australian Lachlan Fold Belt: structural and thermal aspects. *In:* Burg, J.-P. & Ford, M. (eds) *Orogeny Through Time*. Geological Society, London, Special Publications, **121**, 149–177.

Hildreth, W. 1981. Gradients in silicic magma chambers: implications for lithospheric magmatism. *Journal of Geophysical Research*, **86**(B11), 10153–10192.

Hildreth, W. & Moorbath, S. 1988. Crustal contributions to arc magmatism in the Andes of central Chile. *Contributions to Mineralogy and Petrology*, **98**, 455–489.

Huppert, H.E. & Sparks, R.S.J. 1988. The generation of granitic magmas by intrusion of basalt into continental crust. *Journal of Petrology*, **29**, 599–624.

Ireland, T., Flöttmann, T., Fanning, M., Gibson, G. & Preiss, W.V. 1998. Development of the Early Palaeozoic Pacific margin of Gondwana from detrital-zircon ages across the Delamerian Orogen. *Geology*, **26**, 243–246.

Jenkins, R.J. & Sandiford, M. 1992. Observations on the tectonic evolution of the southern Adelaide Foldbelt. *Tectonophysics*, **214**, 27–36.

Keay, S.M., Collins, W.J. & McCulloch, M.T. 1997. A three-component mixing model for granitoid genesis: Lachlan Fold Belt, eastern Australia. *Geology*, **25**, 307–310.

Mancktelow, N.S. 1990. The structure of the southern Adelaide Fold Belt. *In:* Jago, J.B. & Moore, P.S. (eds) *The Evolution of a Late Precambrian–Early Palaeozoic Rift Complex: the Adelaide Geosyncline*. Geological Society of Australia, Special Publication, **16**, 483–495.

Milnes, A.R., Compston, W. & Daily, B. 1977. Pre- to syn-tectonic emplacement of early Palaeozoic granites in southeastern South Australia. *Journal of the Geological Society of Australia*, **24**, 87–106.

Moores, E.M. 1991. Southwest U.S.–East Antarctica (SWEAT) connection: a hypothesis. *Geology*, **19**, 425–428.

Morrison, R.S. & Foden, J.D. 1990. A zoned pluton in the Peake and Dennison Ranges, South Australia: implications to Mid Cambrian magmatism in the Adelaide Geosyncline. *In:* Jago J.B. & Moores, P.S. (eds) *The evolution of a late Precambrian–Early Proterozoic Rift Complex: The Adelaide Geosyncline*. Geological Society of Australia, Special Publications, **16**, 450–464.

Münker, C. & Cooper, R.A. 1995. The island arc setting of a New Zealand Cambrian volcano-sedimentary sequence: implications for the evolution of the SW Pacific Gondwana fragments. *Journal of Geology*, **103**, 687–700.

Münker, C. & Crawford, A.J. 2000. Cambrian arc evolution along the SE Gondwana active margin: a synthesis from Tasmania–New Zealand–Australia–Antarctica correlations. *Tectonics*, **19**, 415–432.

Offler, R. & Fleming, P.D. 1968. A synthesis of folding and metamorphism in the Mt. Lofty Ranges, South Australia. *Journal of the Geological Society of Australia*, **15**, 245–266.

O'Halloran, G.J. & Cas, R.A. 1995. Evidence for syndepositional deformation from the Late Devonian of the Mansfield Basin, east–central Victoria. *Australian Journal of Earth Sciences*, **42**, 581–596.

Oliver, N. & Zakowski, S. 1995. Timing and geometry of deformation, low-pressure metamorphism and anatexis in the eastern Mt Lofty Ranges: the possible role of extension. *Australian Journal of Earth Sciences*, **42**, 501–507.

Perry, F., DePaolo, D. & Baldridge, W.S. 1992. Isotopic evidence for the decline in crustal contributions to caldera-forming rhyolites of the western United States during the middle to late Cenozoic. *Geological Society of America Abstracts*, **23**, A441.

Powell, C.McA., Preiss, W., Gatehouse, C., Krapez, B. & Li, Z. 1994. South Australian record of a Rodinian epicontinental basin and its mid-Neoproterozoic break-up (700 Ma) to form the Palaeo-Pacific ocean. *Tectonophysics*, **237**, 113–140.

Powell, R. 1984. Inversion of the assimilation and fractional crystallisation (AFC) equations: characterization of contaminants from isotope and trace element relationships in volcanic suites. *Journal of the Geological Society, London*, **141**, 447–452.

Preiss, W.V. 1987. *The Adelaide Geosyncline: Late Proterozoic stratigraphy, sedimentation palaeontology and tectonics*. Geological Survey of Australia Bulletin, **53**.

Raheim, A. & Compston, W. 1977. Correlations between metamorphic events and Rb–Sr ages in metasediments and eclogite from western Tasmania. *Lithos*, **10**, 271–289.

Sandiford, M., Foden, J., Zhou, S. & Turner, S. 1992. Granite genesis and the mechanics of convergent orogenic belts with application to the southern Adelaide Fold Belt. *Transactions of the Royal Society of Edinburgh: Earth Sciences*, **83**, 83–93.

Sandiford, M., Oliver, R.L., Mills, K.J. & Allen, R.V. 1990. implications for the metamorphic evolution of the Kanmantoo Group. *In:* Jago, J.B. & Moore, P.S. (eds) *The Evolution of a Late Precambrian–Early Palaeozoic Rift Complex: the Adelaide Geosyncline*. Geological Society of Australia, Special Publication, **16**, 483–495.

Sparks, R.S.J., Huppert, H.E. & Turner, J.S. 1984. The fluid dynamics of evolving magma chambers. *Philosophical Transactions of the Royal Society, London, Series A*, **310**, 511–534.

Stüwe, K., Sandiford, M. & Powell, R. 1993. Episodic deformation and metamorphism in low-*P*, high-*T* terranes. *Geology*, **21**, 829–832.

Sun, S.-s. & McDonough, W.F. 1989. Chemical and isotopic systematics of oceanic basalts: implications for mantle composition and processes. *In:* Saunders, A.D. & Norry, M.J. (eds) *Magmatism in the Ocean Basins*. Geological Society, London, Special Publications, **42**, 313–345.

Turner, S. & Foden, J.D. 1996. Magma mingling in late-Delamerian A-type granites at Mannum, South Australia. *Mineralogy and Petrology*, **56**, 147–169.

Turner, S., Kelley, S.P., VandenBerg, A.H.M., Foden, J., Sandiford, M. & Flöttmann, T. 1996. Source of the Lachlan fold belt flysch linked to convective removal of the lithospheric mantle and rapid exhumation of the Delamerian–Ross fold belt. *Geology*, **24**, 941–944.

Turner, S.P. 1996. Petrogenesis of the late Delamerian gabbroic complex at Black Hill, South Australia: implications for convective thinning of the lithospheric mantle. *Mineralogy and Petrology*, **56**, 51–89.

Turner, S.P., Adams, C.J., Flöttmann, T. & Foden, J.D. 1993b. Geochemical and geochronological constraints on the Glenelg River Complex, western Victoria. *Australian Journal of Earth Sciences*, **40**, 275–292.

Turner, S.P., Foden, J.D. & Morrison, R.S. 1992. Derivation of an A-type magma by fractionation of basaltic magma: an example from the Padthaway Ridge South Australia. *Lithos*, **28**, 151–179.

Turner, S.P., Foden, J.D., Sandiford, M. & Bruce, D. 1993a. Sm–Nd isotopic evidence for the provenance of sediments from the Adelaide Foldbelt and southeastern Australia with implications for crustal growth models. *Geochimica et Cosmochimica Acta*, **57**, 1837–1856.

Von der Borch, C.C. 1980. Evolution of late Proterozoic to early Palaeozoic Adelaide Fold Belt, Australia: comparisons with post-Permian rifts and passive margins. *Tectonophysics*, **70**, 115–134.

Voshage, H., Hofmann, A.W., Mazzucchelli, M., Rivalenti, G., Sinigoi, S., Raczek, I. & Demarchi, G. 1990. Isotopic evidence from the Ivrea zone for a hybrid lower crust formed by magmatic underplating. *Nature*, **347**, 731–736.

White, A.J.R. & Chappell, B.W. 1988. Some supercrustal (S-type) granites of the Lachlan Fold Belt. *Transactions of the Royal Society of Edinburgh: Earth Sciences*, **79**, 169–182.

Williams, I.S., Chappell, B.W., Chen, Y. & Crook, K.A.W. 1992. Inherited and detrital zircons—vital clues to the granite protoliths and early igneous history of southeastern Australia. *Transactions of the Royal Society of Edinburgh: Earth Sciences*, **83**, 503.

Received 25 July 2001; revised typescript accepted 4 February 2002.
Scientific editing by Sally Gibson